

## **An engineered third electrostatic constriction of aerolysin to manipulate heterogeneously charged peptides transport**

Hongyan Niu<sup>a</sup>, Meng-Ying Li<sup>a,b</sup>, Yi-Lun Ying<sup>a,b\*</sup>, Yi-Tao Long<sup>a</sup>

<sup>a</sup> *State Key Laboratory of Analytical Chemistry for Life Science, School of Chemistry and Chemical Engineering, Nanjing University, Nanjing 210023, P. R. China*

<sup>b</sup> *Chemistry and Biomedicine Innovation Center, Nanjing University, Nanjing 210023, P. R. China*

\*Correspondence to: [yilunying@nju.edu.cn](mailto:yilunying@nju.edu.cn)

### **Table of Contents**

#### **Methods**

Reagents and chemicals; Preparation of aerolysin nanopores; Data acquisition and analysis; The measurement of the reversal potential for AeLs; Molecular dynamics simulations; Circular dichroism spectroscopy.

#### **Table S1**

The properties of peptides used in experiments

#### **Figure S1**

SDS-PAGE analysis of WT and mutant proaerolysin

#### **Figure S2**

Statistical analysis of heterogeneously charged peptides at +120 mV with N226Q/S228K AeL

#### **Figure S3**

Determination of the reversal potentials for WT and mutant AeLs

#### **Figure S4**

Electrostatic constricted regions of AeLs.

#### **Figure S5**

Effects of the applied voltages on the duration for A $\beta$ 25-35 with various mutant AeLs

## Methods

### Reagents and chemicals

Tris (hydroxymethyl) aminomethane (Tris) ( $\geq 99\%$ ), EDTA ( $\geq 99\%$ ) were purchased from Aladdin Co., Ltd. (Shanghai, China). KCl ( $\geq 99\%$ ) and decane (anhydrous,  $\geq 99\%$ ) were purchased from Sigma-Aldrich Co., Ltd. (St. Louis, MO). 1, 2-Diphytanoyl-sn-glycero-3-phosphocholine (powder,  $\geq 99\%$ ) was purchased from Avanti Polar Lipids, Inc. (Alabaster, AL). All peptides were purchased from G.L. Biochem. Ltd. (Shanghai, China). All the chemicals used are analytical grade. The aqueous solution in our experiments was prepared with ultrapure water (18.2 M $\Omega$  cm at 25 °C).

### Preparation of aerolysin nanopores

The proaerolysin was prepared according to our previous work.<sup>1</sup> The proaerolysin was treated with trypsin-EDTA to obtain the activated monomers to self-assemble into heptamer. The detailed characterization of aerolysin nanopores is shown in the following Figure S1.

### Data acquisition and analysis

The current traces were recorded with Axon 200B equipped with a Digidata 1440A A/D converter (Molecular Devices, USA). All data were low-pass filtered at 5 kHz and the sampling rate of the instrument was 100 kHz. The data analysis was performed by using Mosaic software<sup>2, 3</sup> and OriginLab 8.0. Durations and frequencies were determined by single exponential fittings. Frequencies were calculated by  $f = 1/\tau_{\text{on}}$ , where  $\tau_{\text{on}}$  represents the interval time between two adjacent events (Figure S2).

### The measurement of the reversal potentials for AeLs

In order to measure the reversal voltage  $V_m$  of aerolysin nanopores, we introduced asymmetrical concentrations in *cis* and *trans* chambers, which were 1 M KCl on the *cis* chamber and 0.2 M KCl on the *trans* side. Firstly, 0.2 M KCl was added into both the *cis* and *trans* chamber of the lipid bilayer. The aerolysin was then added into the *cis* chamber until the nanopores were formed in the lipid bilayer.<sup>4</sup> And the number of nanopores in the lipid bilayer would not influence the measurement of the reversal potential. Then we concentrated the electrolyte solution in the *cis*-compartment to 1 M. Under such asymmetric electrolyte conditions, the current through the nanopore was not zero at zero applied voltage. Then, we measured the reversal voltage  $V_m$  (Figure S3). Agarose salt bridges containing saturated KCl were used between electrodes and buffer solution to ensure the stability of the electrodes. The measurements of the reversal potentials were

using a portable electrochemical instrument named “Cube-D0” and a home-designed software “Smartnanopore”. At  $T = 25\text{ }^{\circ}\text{C}$ , we obtain  $V_m = -11.3\text{ mV}$  for WT AeL and  $V_m = -10.5\text{ mV}$  for N226Q AeL, and  $V_m = -26.2\text{ mV}$  for N226Q/S228K AeL.

Then ion selectivity was calculated by using the Goldman-Hodgkin-Katz equation (equation 1)<sup>5</sup> :

$$V_m = \phi' - \phi'' = \frac{RT}{F} \ln \frac{P_{K^+} [a_{K^+}]_{cis} + P_{Cl^-} [a_{Cl^-}]_{trans}}{P_{K^+} [a_{K^+}]_{trans} + P_{Cl^-} [a_{Cl^-}]_{cis}} \quad \#(1)$$

where  $F$  is the Faraday constant,  $R$  the gas constant, and  $T$  the absolute temperature,  $a_{K^+}$  and  $a_{Cl^-}$  the activity of the  $K^+$  or  $Cl^-$  on either side of the nanopore. Accordingly, the ion selectivities ( $P_{K^+} / P_{Cl^-}$ ) are 0.17, 0.54 and 0.52 of N226Q/S228K AeL, N226Q AeL WT AeL, respectively.

These results demonstrate that the newly designed constricted region R3 is necessary to modulate the ion permeability of AeL. Therefore, the direction of EOF is *cis*-to-*trans* side at a positive voltage which is determinate by the motion of water associated with the enhanced transport of anions across the AeL. Based on the permeability ratios, the velocity of EOF can be calculated using the following equation<sup>6</sup>:

$$v_{EOF} = \frac{J_{\omega}}{\pi r_{pore}^2 C_{\omega}} \quad \#(2)$$

where  $r_{pore}$  is the average radius of the AeL and  $C_{\omega}$  is the number of water molecules per unit volume.  $J_{\omega}$  the number of water molecules flowing through the pore from the *cis* side to the *trans* side per unit time. Assuming the mutant and WT AeLs have the same number of water molecules per unit volume,  $J_{\omega}$  can be estimated by the following equation:

$$J_{\omega} = N_{\omega} \frac{I}{e} \left( \frac{1 - P_{K^+} / P_{Cl^-}}{1 + P_{K^+} / P_{Cl^-}} \right) \quad \#(3)$$

where  $N_{\omega}$  is the number of water molecules transported per ion,  $I$  the ionic current and  $e$  the elementary charge.

## Molecular dynamics simulations

**Model Construction.** The model of N226Q/S228K mutant aerolysin was based on the WT AeL, which has been reported by our previous work<sup>7</sup>. The N226Q/S228K AeL was constructed by using Mutator Plugin in VMD<sup>8</sup>.

**System Equilibrium.** The detailed equilibrium of aerolysin system refers to our previous work. After system equilibration, 30-ns simulations with an electric field applied to N226Q/S228K AeL system were performed as an NVT ensemble without any positional restrain applied to the aerolysin side chain to simulate the application of a voltage bias of +120 mV. Then the electrostatic potential map of each system was computed based on the last 10 ns simulation trajectory using the PME electrostatics plugin of VMD according to the procedure described in previous study.<sup>7</sup> The average diameter was calculated by the HOLE<sup>9</sup>.

#### **Circular dichroism spectroscopy**

Circular dichroism spectroscopy (CD) experiments were performed on Applied Photophysics Chirascan (Applied Photophysics, England). Peptides were dissolved to 1 mg/mL with 1 M KCl. Spectra were generally recorded over the wavelength range of 180-260 nm.

**Table S1 The properties of heterogeneously charged peptides**

Peptide	Sequence	Isoelectric point <sup>a</sup>	Molecular weight	Net Charge <sup>b</sup>
A $\beta$ 35-25	MLGIIAGKNSG	10.09	1060.26	+1
A $\beta$ 25-35	GSNKGAIIGLM	10.09	1060.26	+1
A $\beta$ 5-16	RHDSGYEVHHQK	7.98	1492.55	0
A $\beta$ 35-25D4	MLGIIAGKNSGDDDD	3.42	1520.61	-3

<sup>a</sup> The isoelectric points of examined peptides are calculated from [http://www.novopro.cn/tools/calc\\_peptide\\_property.htm](http://www.novopro.cn/tools/calc_peptide_property.htm)

<sup>b</sup> The net charges of examined peptides are calculated from [http://www.novopro.cn/tools/calc\\_peptide\\_property.htm](http://www.novopro.cn/tools/calc_peptide_property.htm)

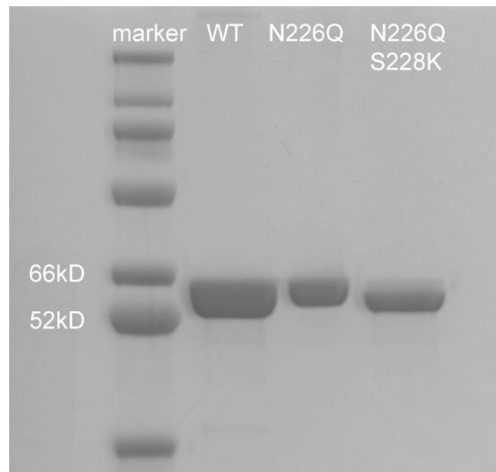


**Figure S1** SDS-PAGE analysis of WT and mutant proaerolysin. Left: WT AeL; middle: N226Q AeL; right: N226Q/S228K AeL.

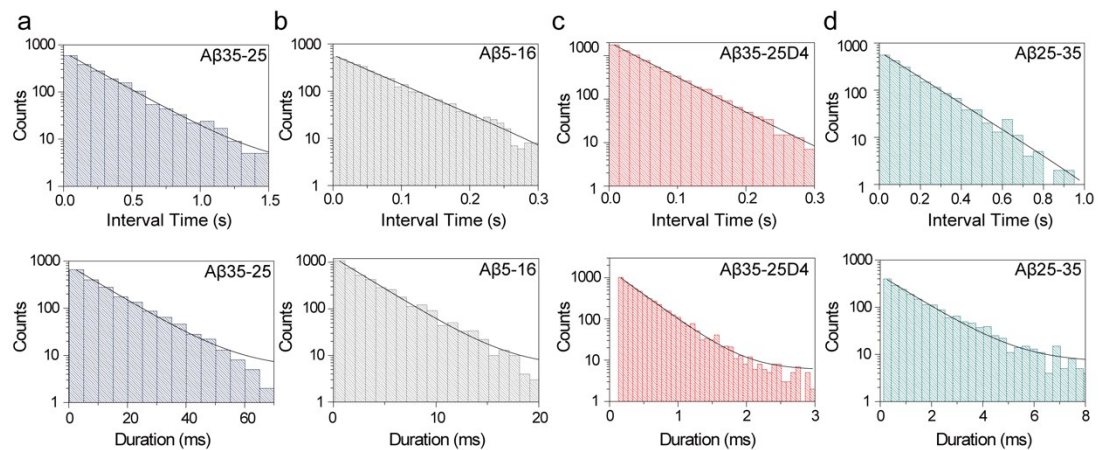


**Figure S2** Statistical analysis of heterogeneously charged peptides at +120 mV with N226Q/S228K AeL. From left to right: (a) A $\beta$ 35-25; (b) A $\beta$ 5-16; (c) A $\beta$ 35-25D4; (d) A $\beta$ 25-35. Interval time histograms and duration histograms were all fitted with exponential distribution. All data were acquired in the electrolyte solution of 1.0 M KCl, 10.0 mM Tris and 1.0 mM EDTA at pH 8.0.

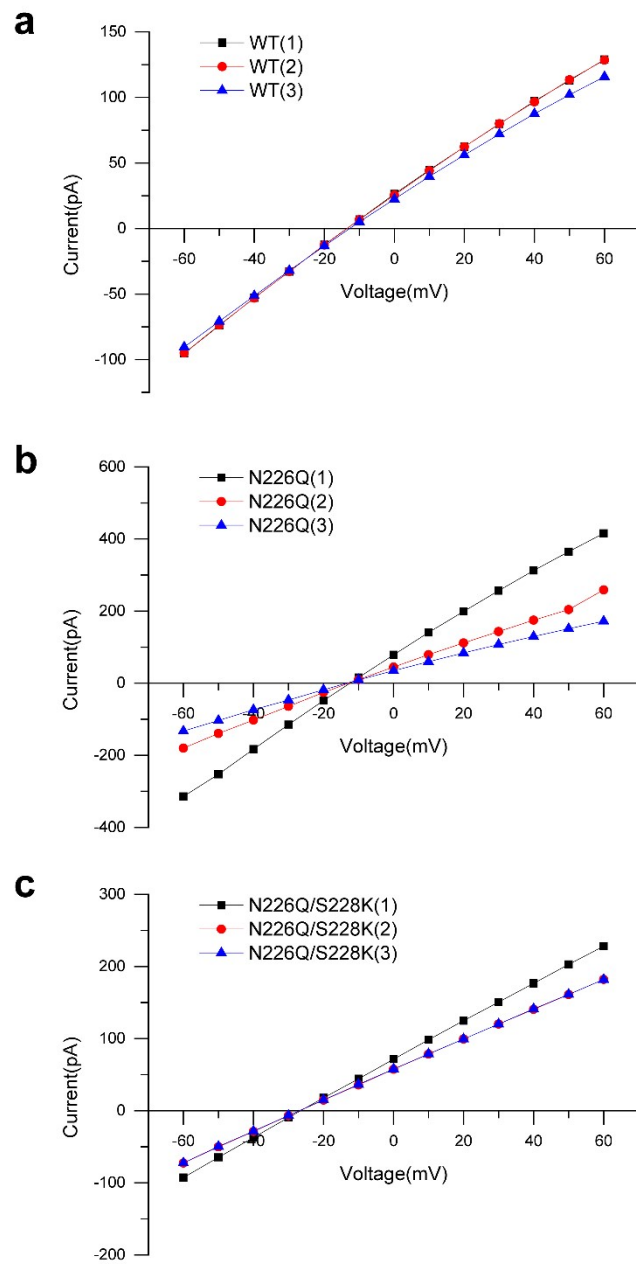


**Figure S3** Determination of the reversal potentials of WT AeL (a), N226Q AeL (b) and N226Q/S228K AeL (c), respectively. Noted that the numbers of nanopores do not influence the reversal potential.

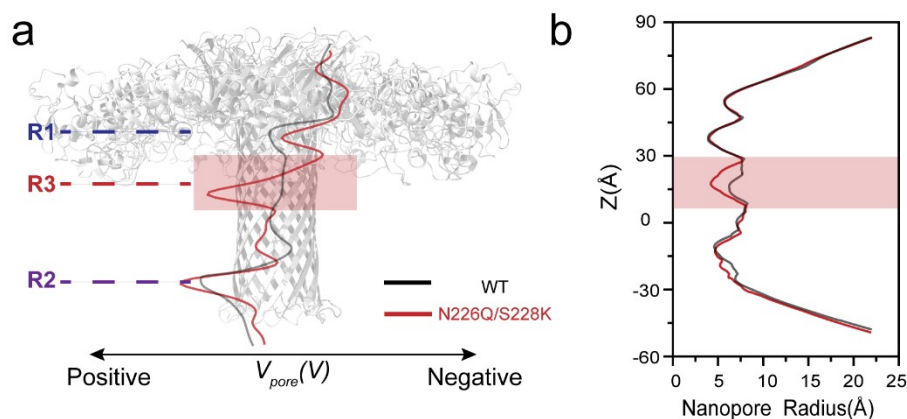


**Figure S4** Electrostatic constricted regions of AeLs. (a) Three constricted regions of WT AeL. The red band represents the R3 (N226Q, S228K) region. The other two constrictions (R1 around R220 and R2 around K238) are also marked here, respectively. The red and black lines are electrostatic potential distributions along the WT AeL (black) and N226Q/S228K AeL (red) at + 120 mV, respectively. (b) The radius of WT AeL (black) and N226Q/S228K AeL (red), respectively.

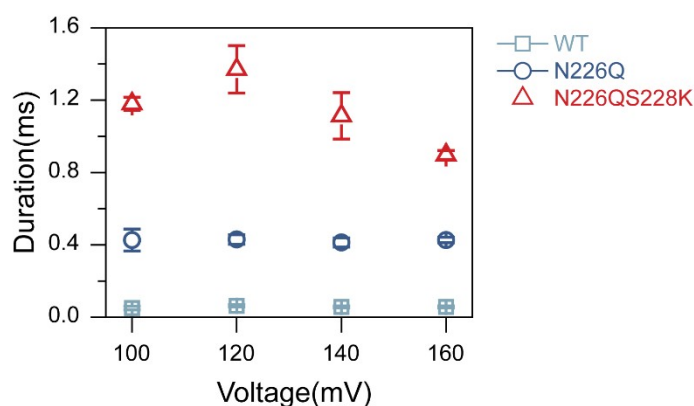


**Figure S5** Effects of the applied voltages on the duration for A $\beta$ 25-35 with WT AeL (light blue, square), N226Q AeL (dark blue, circle) and N226Q/S228K AeL (red, triangle), respectively.

#### Reference:

1. Y.-Q. Wang, M.-Y. Li, H. Qiu, C. Cao, M.-B. Wang, X.-Y. Wu, J. Huang, Y.-L. Ying and Y.-T. Long, *Anal. Chem.*, 2018, **90**, 7790-7794.
2. J. H. Forstater, K. Briggs, J. W. F. Robertson, J. Ettetdgui, O. Marie-Rose, C. Vaz, J. J. Kasianowicz, V. Tabard-Cossa and A. Balijepalli, *Anal. Chem.*, 2016, **88**, 11900-11907.
3. A. Balijepalli, J. Ettetdgui, A. T. Cornio, J. W. F. Robertson, K. P. Cheung, J. J. Kasianowicz and C.

- Vaz, *ACS Nano*, 2015, **9**, 12583-12583.
4. M. Boukhet, F. Piguet, H. Ouldali, M. Pastoriza-Gallego, J. Pelta and A. Oukhaled, *Nanoscale*, 2016, **8**, 18352-18359.
  5. R. Benz and T. Chakraborty, in *Methods in Neurosciences*, ed. P. M. Conn, *Academic Press*, 1992, **8**, 1-14.
  - 6 F. Piguet, F. Discala, M.-F. Breton, J. Pelta, L. Bacri and A. Oukhaled, *J. Phys. Chem. Lett.*, 2014, **5**, 4362-4367.
  7. M.-Y. Li, Y.-L. Ying, J. Yu, S.-C. Liu, Y.-Q. Wang, S. Li and Y.-T. Long, *JACS Au*, 2021, **1**, 967-976.
  8. A. Aksimentiev and K. Schulten, *Biophys. J.*, 2005, **88**, 3745-3761.
  9. O. S. Smart, J. G. Neduelil, X. Wang, B. A. Wallace and M. S. P. Sansom, *J. Mol. Graph. Model.*, 1996, **14**, 354-360.